

Transformer Bushing Temperature Measurement Model Based on Infrared Temperature Measurement

Chen Gu¹, Yu Yin¹, Qinyu Pan¹, Min Xu¹, Wangwang Shi², Guifeng Wu², and Donglei Chen²

¹State Grid Yangzhou Power Supply Company, Yangzhou 225000 China

²Hydraulic and Energy Engineering College of Yangzhou University, Yangzhou 225127, China

Keywords: Transformer bushing; early warning; infrared temperature measurement; support vector regression (SVR)

Abstract: This paper proposes a new method of temperature measurement and predict model for transformer bushing based on support vector regression (SVR) algorithm. In this model, infrared image is used to measure the temperature of bushing porcelain. Aiming at the phenomenon that the temperature of infrared thermal image is easily disturbed by environment, a SVR filtering method is proposed to correlate the load current with the temperature of infrared thermal image, which maintained the correlation between bushing porcelain temperature and load current, reduced infrared temperature measurement noise. Compared with RBF neural network, BP neural network and SVR method, the training and prediction results of 110kV transformer bushing in a sample city show that the model has better prediction ability.

1. Introduction

Transformer bushing is one of the important parts of power transformer. Bushing plays the role of insulating ground, supporting lead and isolating external. At the same time, it leads the high and low voltage lead inside transformer to the outside of oil tank. It is the channel for transformer to exchange energy between inside and outside. The sealing performance, electrical strength, mechanical structure and thermal stability of bushing have an important impact on the operation of transformer, and the requirement for electrical strength and mechanical strength of bushing is high in the field. Common faults of casing mainly include terminal screen discharge, heating of casing joint, water intake and dampness of casing, etc[1],if the casing can not be eliminated in time, it will often lead to very serious consequences. Although there are many kinds of casing faults, most of them will show temperature faults. Casing heating faults are generally divided into two types: current heating faults and voltage heating faults.[2]The main reasons for the current-type heating failure of bushing are that the processing and installation technology does not meet the requirements or the contact resistance becomes larger due to conductor oxidation, etc. The voltage-type heating failure of bushing is mainly caused by poor insulation of conductive rod induced by bushing, which will produce an unbalanced magnetic field to bushing porcelain bushing, resulting in abnormal voltage distribution and heating failure caused by the increase of leakage current. The oil seepage fault of casing also shows that the temperature of casing is too high or obvious temperature gradient.

Infrared temperature measurement technology has been widely used in live detection of power equipment, and it is also one of the routine live detection items of transformers. Infrared temperature measurement can successfully detect various heating defects of transformers, including dielectric loss heating of high voltage bushing, abnormal oil level in bushing, poor contact between bushing joints, magnetic leakage heating of the main body, etc.Literature [3] gives the key points of infrared accurate temperature measurement for diagnosis of oil shortage in bushing, discusses the effectiveness and accuracy of infrared temperature measurement results in judging the internal and external defects of equipment, and successfully eliminates a major potential safety hazard of main transformer. Literature [4] discussed the error of infrared temperature measurement caused by the interference of air thermal convection in the isolation wall, and put forward the method to prevent

misjudgment. The temperature rise of casing is related to the current and environmental parameters flowing through the casing. Document [5] studies the temperature change curves of top oil temperature, bottom oil temperature, insulator and metal conductor of casing from the point of view of temperature field, but this method is difficult to realize in real-time monitoring and early warning. With the increase of the amount of on-line monitoring device for casing, the analysis of monitoring data has increased dramatically. It is necessary to automatically predict the state of equipment through accurate and effective early warning strategy. The online monitoring system and early warning strategy of casing dielectric loss are studied in literature [6-8], and the relationship between dielectric loss and environment is analyzed. Casing temperature early warning and fault diagnosis technology based on infrared imaging has also begun to be applied [9-10].

The core of temperature-based early warning technology is temperature modeling. Because the factors affecting the temperature of transformer and bushing are many and complex, artificial intelligence methods are often used to solve engineering problems, such as neural network method, fuzzy mathematics theory, support vector machine (SVM), etc. [11-12]. SVM is an advanced intelligent supervised learning classification method based on statistical theory. It improves the generalization ability of learning machine by seeking the smallest structured risk and minimizes the empirical risk and confidence interval. It has excellent performance in solving the fitting problem of high-dimensional non-linear functions with small samples.

2. Implementation of SVR Algorithm

Support Vector Regression (SVR) method maps input samples into high-dimensional feature space H through non-linear mapping $\varphi(x)$, so that linear regression functions can be established in H space by using structural risk minimization principle.

$$y' = w \cdot \varphi(x) + b \quad (1)$$

In the formula, y' is the predicted value, W is the weight vector and B is the bias value.

The implementation of SVR is based on the introduction of error threshold ε and relaxation factors ξ_i and ξ_i^* . By using the principle of structural minimization, the fitting problem is transformed into the following optimization problem, that is, equation (2)

$$\begin{cases} \min \frac{1}{2} \|w\|^2 + C \sum_{i=1}^l (\xi_i + \xi_i^*) \\ \text{s.t. } y_i - w \cdot \varphi(x) - b \leq \varepsilon + \xi_i \\ w \cdot \varphi(x) + b - y_i \leq \varepsilon + \xi_i^* \\ \xi_i, \xi_i^* \geq 0 \end{cases} \quad (2)$$

$C > 0$ is the penalty factor. In order to solve equation (2), duality principle can be used to convert it into the following optimization problems, see equation (3).

$$\begin{cases} \max \left\{ -\frac{1}{2} \sum_{i,j=1}^l (\alpha_i - \alpha_i^*)(\alpha_j - \alpha_j^*) K(x_i, x_j) - \right. \\ \left. \varepsilon \sum_{i=1}^l (\alpha_i + \alpha_i^*) + \sum_{i=1}^l y_i (\alpha_i - \alpha_i^*) \right\} \\ \text{s.t. } \sum_{i=1}^l (\alpha_i - \alpha_i^*) = 0, \alpha_i, \alpha_i^* \in [0, C] \end{cases} \quad (3)$$

From this, the nonlinear regression function of SVR can be obtained.

$$y' = \sum_{i=1}^l (a_i - a_i^*) K(x_i, x_j) + b \quad (4)$$

In the formula $K(x_i, x_j)$ satisfies Mercer's condition, the commonly used kernels include the radial basis function. That is

$$k(x_i, y) = \exp(-\gamma \|x_i - y\|^2) \quad (5)$$

The polynomial kernel function is

$$k(x_i, y) = (x_i^T y + b)^d$$

And the sigmoid kernel function is

$$k(x_i, y) = \tan(x_i^T y + v)$$

3. Casing Temperature Rise Modeling and SVR Implementation

3.1. Casing Temperature Rise Model.

The heat inside the casing is dissipated by heat conduction, convection and radiation. Different heat dissipation modes have their own laws and characteristics. According to the simulation theory, if the differential equation forms of the two physical phenomena are identical, and the boundary conditions and geometric shapes of the two carriers are similar, the analytical and experimental solutions of the two equations have the same mathematical form. Thermoelectric analogy is based on Simulation theory, analogizing thermal parameters with electrical parameters which are similar in mathematical definitions. According to the corresponding relationship of parameters, the thermal circuit law is analogized by circuit law. Thermoelectric circuit model in transformer is transformed into circuit model. Fig. 1 is the heat flow pattern of bushing.

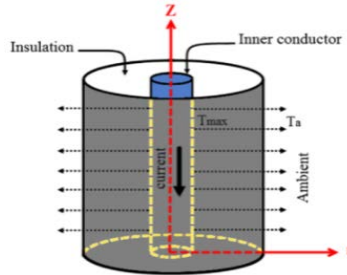


Fig. 1 The heat flux direction in the bushing.

When the transformer is running, the heat source of the bushing is mainly the loss of current-carrying conductor and the dielectric loss of the capacitor core in the bushing. The heat generated by the loss of current-carrying conductor is first transmitted to the surface of the conductor through conduction. The heat from the surface of the bushing is realized by convection in the oil, and then the heat from the oil is transferred to the inner wall of the bushing ceramics through convection; the heat generated by the dielectric loss of the capacitor core. It is transported to the surface and convection to the inner wall of ceramics. Because of the thin core and small heat capacity, the transfer process can be neglected. The heat from the inner wall is transferred to the outer wall through heat conduction. Finally, all the heat is radiated and convective from the outer wall of the tank and ceramic to the surrounding air. The heat flow in the process is similar to the current flow in the circuit. The equivalent heat circuit model is shown in Figure 2.

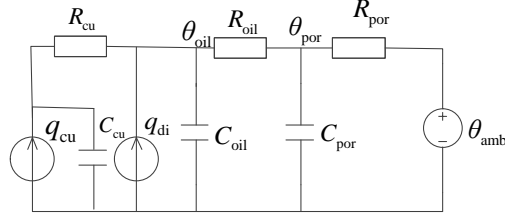


Fig. 2 The dynamic thermal circuit model for bushing

In Figure 2, q_{cu} and q_{di} are the current-carrying conductor loss and the dielectric loss of the capacitor core of the casing respectively, which are expressed by ideal heat source. R_{cu} , R_{oil} and R_{por} are respectively the non-linear thermal resistances of current-carrying conductors to oil, oil to ceramics and ceramic walls to external air. The heat capacities of C_{cu} , C_{oil} and C_{por} are current-carrying conductors, oil and ceramic walls, respectively, θ_{oil} , θ_{por} , θ_{amb} are oil temperature, ceramic wall temperature and ambient temperature, respectively. For the current-carrying conductor, the temperature rise is faster than that of oil and ceramic wall, and its transient process can be neglected. The differential equations of the simplified model can be obtained from Fig. 2, which are expressed by equation (9):

$$\begin{cases} q_{cu} + q_{di} = C_{oil} \frac{d\theta_{oil}}{dt} + \frac{\theta_{oil} - \theta_{por}}{R_{oil}} \\ 0 = C_{por} \frac{d\theta_{por}}{dt} + \frac{\theta_{por} - \theta_{amb}}{R_{por}} - \frac{\theta_{oil} - \theta_{por}}{R_{oil}} \end{cases} \quad (6)$$

3.2. SVR Prediction Model.

With the help of infrared thermometry, the measured ceramic wall temperature θ_{por} is used as the monitoring and predicting variable. It can be obtained from formula (6) that the system with variable θ_{por} is the second-order system, which is related to current-carrying conductor loss, dielectric loss of capacitor core, environmental conditions and other factors. The loss of current-carrying conductor is related to casing current, while dielectric loss is related to voltage. Therefore, the load current, voltage, ambient temperature, ambient humidity of casing and ceramic wall temperature at the first two sampling times are chosen as the choices in this paper. The structure of the input variable and the output variable, the ceramic wall temperature at the current time, is shown in Figure 2.

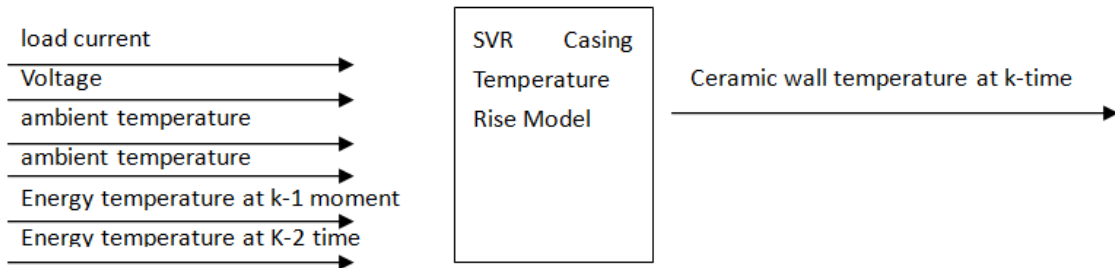


Fig. 3 SVR temperature structure for bushing

3.3. Preprocessing of Infrared Measurement Data.

In the process of model training and prediction, the normalization of data is very important to improve the convergence and generalization ability of the model, because the input and output parameters of casing vary greatly, and data need to be preprocessed. The normalization formula is shown in (10):

$$x^* = \frac{x - x_{\min}}{x_{\max} - x_{\min}} \quad (6)$$

In the formula, x^* is the normalized value, x is the sample data, x_{\min} is the minimum of the sample data and x_{\max} is the maximum of the sample data. Infrared temperature measurement results are greatly influenced by external factors. The measurement results are disturbed greatly and contain high frequency component noise. This noise has great influence on the accuracy of training and prediction. Usually low-pass filter is used to filter out the noise, but the output data of low-pass filter is delayed, which makes the output of filtered filter not synchronized with other data. At the same time, in the case of less data, because of the fact that the output of low-pass filter is not synchronized with other data. The data of filtering transition process is not suitable for SVR learning, which further reduces the amount of data, thus affecting the training and learning accuracy. In this paper, the radial basis function (RBF) kernel SVR is used to filter, which can eliminate the above unfavorable factors, that is, the input parameter of SVR is time and the output is θ_{por} . In order to filter with radial basis function SVR, ε and C in formula (3) need to be determined, and γ in Formula (5). Formula (6) shows that θ_{por} is greatly influenced by q_{cu} , while q_{cu} is proportional to the square of load current. In order to determine the above SVR filtering parameters, this paper uses load current I_L and θ_{por} to carry out SVR filtering at the same time, specifically as follows: Firstly, SVR filter is applied to the square I_L^2 of the load current to ensure that the filtered $I_{L_f}^2$ and I_L^2 curves almost coincide, and ε , C and γ are determined. The above parameters are applied to the SVR filtering of θ_{por} , so that the filtered I_L^2 can reflect the influence of load current. Fig. 4 shows the current curve of square root after SVR filtering. It can be seen that the load current almost coincides before and after SVR filtering. Fig. 5 shows the temperature curve of the ceramic wall of casing with the parameters in Fig. 4. It can be seen that the curve after I_L^2 SVR filtering is smoother than the original data curve.

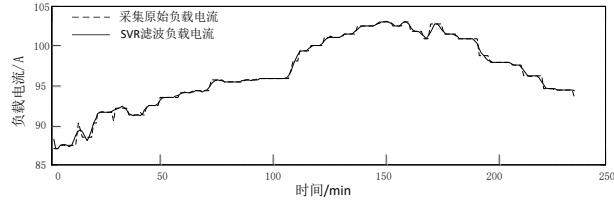


Fig. 4 SVR filtered current through bushing

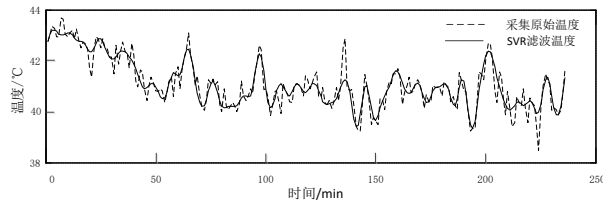


Fig. 5 SVR filtered porcelain temperature for bushing

4. Example Analysis

In this paper, the voltage, current, ambient temperature and humidity of a 110kV substation in Yangzhou are monitored in real time. The sampling interval is 1 minute, and the casing temperature is monitored synchronously by infrared thermal imager. There are 236 sample data, the first half is used for model training and the second half is used for prediction. Six variables, load current,

voltage, ambient temperature, ambient humidity and ceramic wall temperature at the first two moments, were used as input of the SVR model, and the ceramic wall temperature was filtered by SVR.

In order to compare the performance of the SVR temperature model proposed in this paper, feedforward BP neural network and RBF neural network are used to model, and the same sample set is trained and predicted. The RBF kernel function is used in the SVR model. After repeated parameter optimization, C and gamma satisfying the requirements are 4.0 and 0.15, respectively. The number of nodes in input layer, hidden layer and output layer of BP network is 6, 15 and 1, respectively. Tansig function is used for transfer function of hidden layer, logsig function is used for transfer function of output layer, Levenberg-Marquardt algorithm is used for training function, learning rate $Lr=0.01$, and target error $Eg=0.001$. Fig. 6 is the original data and training output results under three models, Fig. 7 is the training output error of three models, Fig. 8 is the original data and the prediction output results under three models, and Fig. 9 is the prediction output error of three models. As can be seen from the above figure, the training error of RBF network is very small, but the prediction error is large, which shows that its generalization ability is poor; BP network and SVR model have better generalization ability, and SVR has smaller error, which shows that the model in this paper is more suitable for casing temperature modeling and temperature prediction.

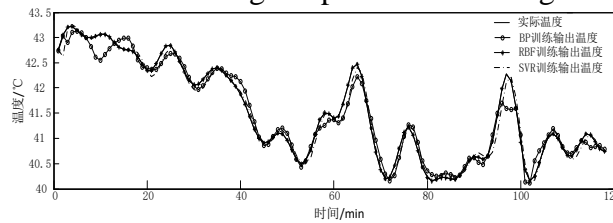


Fig. 6 Curves of training results

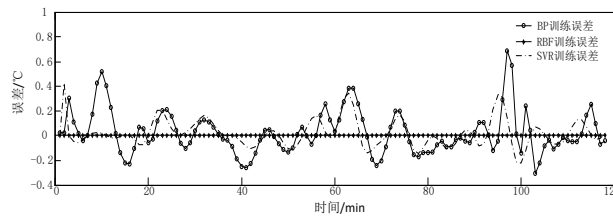


Fig. 7 Error curves of training results

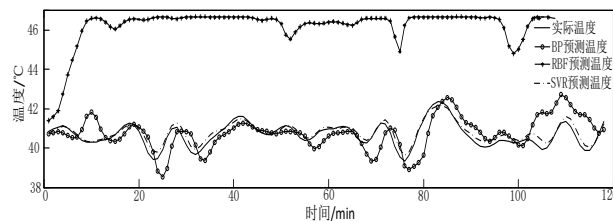


Fig. 8 Curves of predicted results

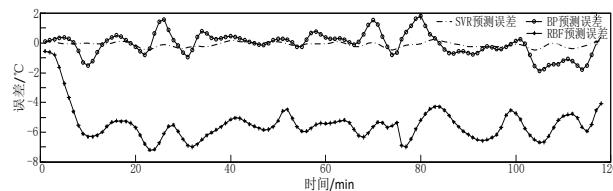


Fig. 9 Error curves of predicted results

5. Conclusion

In this paper, a transformer bushing temperature measurement model based on SVR algorithm is proposed. Infrared image is used to measure the ceramic wall temperature of bushing. In view of the fact that the temperature formed by infrared thermal image is susceptible to external interference,

SVR filtering is proposed for the square of the load current first, and then SVR filtering for the infrared thermal image temperature is carried out for the parameters determined by SVR filtering, the correlation between casing temperature and load current is maintained, and the infrared temperature measurement noise is eliminated. Through the analysis of heat transfer process of casing, the heat circuit model of casing and the corresponding differential equation are established. On this basis, six variables of load current, voltage, ambient temperature, ambient humidity and ceramic wall temperature at the first two moments are used as input of SVR model to model casing temperature. The model is trained by using actual casing operation data, and the RBF neural network and BP network are used to train the model. The comparison between neural network and SVR method proves that the proposed casing temperature has better prediction accuracy and SVR model has better generalization ability. A new U is proposed for indirect calculation of transformer casing temperature and temperature early warning during operation.

References

- [1] Analysis of common defects and faults in transformer bushing of Chen Liangyuan, Li Dajian, Zhao Jian. 110 kV and above [J].Guangxi Electric Power, 2017,40(3):30-35.
- [2] Yao Liuliang. Fault analysis and treatment of power transformer bushing [J].March 2017: 48-49.
- [3] Mali, Hu Xiaobin, Zhang Jung. Analysis of Oil Defect in Main Transformer Bushing Diagnosed by Infrared Precise Temperature Measurement [J], Jiangxi Electric Power, 2016 (6): 46-48
- [4] Liu Liansheng, Jiao Hongtao. Case analysis of infrared temperature measurement defects in transformer bushing [J].2018, Vol. 21, No. 1: 13-15.
- [5] Zhenbing Zhao, Guozhi Xu, Yincheng Qi, An Intelligent On-Line Inspection and Warning System Based on Infrared Image for Transformer Bushings, Recent Advances in Electrical & Electronic Engineering, 2016 (9), PP. 53-62.
- [6] Xia Jian, Ding Weidong, Sun Xudong. Research on new online monitoring and early warning strategy of Transformer Bushing Based on data analysis [J].High Voltage Electrical Appliances, 2018, 54 (9): 0171-0176.
- [7] Li Feng, Sun Xudong, Wang Hongbin, Xia Jian. Transformer bushing dielectric loss monitoring and early warning strategy considering meteorological environmental impact [J]. High voltage electrical appliances, 2017, 53 (7): 0159-0166.
- [8] Ricardo Manuel Arias Velsquez, Jennifer Vanessa Meja Lara, Bushing failure in power transformers and the influence of moisture with the spectroscopy test, Engineering Failure Analysis, Vol. 94, PP. 300-312, 2018.
- [9] N. S. Jyothi, T. S. Ramu and Manoj Mandlik. Temperature Distribution in Resin Impregnated Paper Insulation for Transformer Bushings, IEEE Transactions on Dielectrics and Electrical Insulation Vol. 17, PP. 931-938, 2010
- [10] T. Mariprasath, V. Kirubakaran, A real time study on condition monitoring of distribution transformer using thermal imager, Infrared Physics & Technology, Vol. 90, PP. 79-85, 2018.
- [11] Peng Daogang, Chen Yuewei, Qian Yuliang, Huang Chao. Soft-sensing model of transformer winding temperature based on particle swarm optimization and support vector regression [J].Journal of Electrical Technology, Vol.33 No.8:1742-1749
- [12] Chen Weigen, Teng Li, Liu Jun, et al. Transformer winding hot spot temperature prediction model based on genetic optimization support vector machine [J]. Journal, 2014, 29 (1): 44-50.